MOLECULAR AND CELLULAR BIOLOGY, Oct. 1993, p. 5990–5998
0270-7306/93/105990-09$02.00/0

Vol. 13, No. 10

A U3 Small Nuclear Ribonucleoprotein-Requiring Processing Event in the 5′ External Transcribed Spacer of *Xenopus* Precursor rRNA

EDWARD B. MOUGEY, LOUISE K. PAPE,† AND BARBARA SOLLNER-WEBB*

Department of Biological Chemistry, The Johns Hopkins University School of Medicine, 725 North Wolfe Street, Baltimore, Maryland 21205

Received 18 May 1993/Returned for modification 21 June 1993/Accepted 24 June 1993

A processing site has been identified within the 5′ external transcribed spacer (ETS) of *Xenopus laevis* and *X. borealis* pre-RNAs, and this in vivo processing can be reproduced in vitro. It involves a stable and specific association of the pre-rRNA with factors in the cell extract, including at least four RNA-contacting polypeptides, yielding a distinct complex that sediments at 20S. Processing also requires the U3 small nuclear RNA. This processing, at residue +105 of the 713-nucleotide *X. laevis* 5′ ETS, is highly reminiscent of the initial processing cleavage of mouse pre-rRNA within its 3.5-kb 5′ ETS, previously thought to be mammal specific. The frog and mouse processing signals share a short essential sequence motif, and mouse factors can faithfully process the frog pre-rRNA. This conservation suggests that this 5′ ETS processing site serves an evolutionarily selective function.

The 18S, 5.8S, and 28S RNAs of the ribosome are initially transcribed as a single, large precursor molecule that is then processed to yield the mature species. Major processing sites of metazoan pre-rRNA, originally identified by mapping relatively abundant rRNA processing intermediates in frogs, mice, and humans (8, 35, 36), were concluded to be at the ends of the mature rRNA regions, with the order of cleavage frequently but not obligatorily progressing 5′ to 3′ along the pre-rRNA (arrows in Fig. 1) (reviewed in reference 30). The transcribed spacer regions that separate the mature rRNA segments evidently are degraded rapidly following their excision. Although it was initially thought that the 5′ external transcribed spacer (ETS) was removed from the pre-rRNA in one step, the first processing cleavage in the maturation of mouse pre-rRNA was then found to be at position +650 within the 5′ ETS, ~3 kb upstream from the 18S region (arrowhead in Fig. 1) (11, 20). The mouse 5′ ETS processing region specifically associates with a number of polypeptides, directing the assembly of an ~20S complex (14), and processing also requires the U3 small nuclear ribonucleoprotein (snRNP) (15). The 200-nucleotide (nt) segment just downstream from the processing site is ~85% conserved in sequence in various mammalian species. Processing at analogous positions (400 to 800 nts beyond the initiation site) also occurs in humans, rats, and Chinese hamsters (13, 31, 33). The mouse 5′ ETS processing signal is in the proximal 120 nts of this conserved region, the first ~11 nts being the residues most critical for processing (6, 7).

The 5′ ETSs of mammals are 3 to 4 kb in length, but the 5′ ETSs of most other eukaryotes are much shorter. In various *Xenopus* species, the 5′ ETS is 600 to 750 nts in length; therefore, the upstream processing site of the 18S rRNA region in frogs is the same distance from the 5′ end of the transcript as is the 5′ ETS processing site in mammals (Fig. 1). This fact raises the question of whether mammalian-type 5′ ETS processing involving the formation of a large complex is restricted to mammals or can occur in other eukaryotes. Notably, *Xenopus laevis* oocytes have been reported not to show analogous processing in their 5′ ETS (27).

In this article, we demonstrate that *X. laevis* pre-rRNA shows 5′ ETS processing that is highly analogous to that of mouse pre-rRNA. This *Xenopus* processing occurs both in vivo and in vitro and requires the U3 snRNP. Also, as in mice, the frog processing signal forms a specific ~20S complex with factors in the frog cell extract. Furthermore, the frog processing site is just upstream of a 120-nt *Xenopus* conserved element, the proximal 11 nts of which are essential for processing and are also found at the same position relative to the mammalian processing site. Indeed, the *Xenopus* processing and mouse processing are so similar that the frog signal is faithfully recognized by mouse cell factors. We conclude that this kind of large complex-forming, U3-requiring 5′ ETS processing occurs considerably more widely in eukaryotic evolution than was previously appreciated.

MATERIALS AND METHODS

Plasmid constructs. X293 was generated by inserting *X. laevis* rDNA (genes coding for rRNA) residues +28 to +293 (a *Nar*I fragment from rDNA clone pXlr14a [29]) into the *Acc*I site of pGEM3, downstream from the T7 promoter. The 11-nt block conserved between frogs and mammals (see Fig. 3A) extends from residues +112 to +122 of *X. laevis* rRNA. X293Δl is a derivative of X293 in which rDNA residues +105 to +119 were deleted by Bal 31-S1 nuclease digestion, starting from the *Pvu*I site at residue +113 (partial digestion); this step was followed by recircularization of the plasmid. X293Δr is a derivative of X293 in which residues +113 to +134 were deleted by insertion of a *Sma*I-*Not*I fragment (residues +135 to +177) in place of a *Pvu*I (blunted)-*Not*I fragment (residues +113 to +177). X729, X755, X782, and X811 are analogous to X293, except that they contain a longer region of rDNA extending through the indicated rDNA residue. They were generated by removing from X293 the fragment starting at rRNA residue +177 (*Not*I

* Corresponding author.
† Present address: Department of Chemistry, New York University, New York, NY 10003.

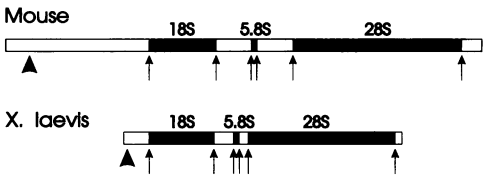

FIG. 1. pre-RNAs of mice and *X. laevis*. The 13.3-kb mouse pre-RNA and the 7.8-kb *X. laevis* pre-rRNA are shown. The 5' ETSs are 4 kb and 713 nts long in mice and *X. laevis*, respectively. Processing sites long known to be involved in rRNA maturation are indicated by arrows (taken from reference 31). The 5' ETS processing site in mouse pre-rRNA, at residue 650, is represented by the arrowhead in the upper diagram. The 5' ETS processing site in *X. laevis* pre-rRNA, at residue 105, shown in this study, is represented by the arrowhead in the lower diagram. The solid boxes indicate the mature rRNA regions.

site) and extending through the downstream polylinker (blunted *Pst*I site) and replacing it with a fragment from pXlr14a extending from residue +177 (*Not*I site) to the indicated downstream rRNA position (exonuclease III-S1 nuclease deletions from an *Xba*I site). X729Δl and X729Δr were formed by replacing the fragment extending from the upstream polylinker (*Eco*RI site) through residue +177 (*Not*I site) of X729 with the corresponding regions from X293Δl and X293Δr, respectively. All deletion endpoints were determined by sequence analysis (17). See Fig. 3B for the transcripts of most of these constructs.

X. borealis subclone Xb392 was formed by inserting residues +7 to +392 (*Stu*I-*Bss*HII fragment; blunted) of *X. borealis* rDNA into the *Sma*I site of pGEM3, downstream from the T7 promoter. Mouse rDNA subclones in pGEM, from which T7 RNA polymerase generates transcripts containing the rRNA segments from residues 546, 645, or 669 to residues 874, or 1294, were described previously (14).

S1 nuclease analysis. RNA was prepared from logarithmically growing cultures of *X. laevis* kidney cells and from *X. laevis* or *X. borealis* stage-6 oocytes. About 12 μg of this RNA or the RNA from one processing reaction was hybridized to 40 fmol of a strand-separated probe and treated with S1 nuclease as described previously (23, 28), and the products were analyzed on a 9 M urea–8% polyacrylamide gel. The *X. laevis* ETS probe corresponds to the 5' portion of the X293 transcript, an *Eco*RI-*Not*I fragment, 5' labeled at the *Not*I site at rRNA residue +177. The *X. borealis* ETS probe is the analogous fragment from Xb392, 5' labeled at the *Not*I site at residue +194. The Maxam-Gilbert (17) sequencing marker lane of the probe DNA migrates 1.5 nts faster than the corresponding fragment generated by S1 nuclease digestion (29).

In vitro processing reaction and complex formation. These studies used an S-100 extract of log-phase *X. laevis* kidney cells (line Xl-K2) that were propagated in tissue culture (19) or an S-100 extract of log-phase mouse tissue culture cells (14).

The substrate and competitor RNAs were transcribed from the T7 promoter of the appropriately cleaved plasmid and gel isolated as described previously (14). The *X. laevis* and *X. borealis* rRNA templates were linearized at the *Hin*dIII site in the polylinker downstream of the rDNA region. The mouse rRNA templates were linearized with *Ava*II at position 875 of the rRNA sequence for the experiments shown in Fig. 6D, 6E, 7B, and 7C and with *Hin*dIII in the polylinker just beyond position 1294 for the experiments shown in Fig. 6C and 7A. Unless otherwise indicated, the substrate RNAs were labeled with ^{32}P and the competitor RNAs were labeled with ^{3}H, the latter for quantitation.

The 25-μl frog processing reaction mixtures contained a final concentration of 20 mM *N*-2-hydroxyethylpiperazine-*N'*-2-ethanesulfonic acid (HEPES) (pH 7.9)–120 mM KCl–2 mM $MgCl_2$–9% glycerol–2 mM dithiothreitol–0.14 mM EDTA–1.5 mM ATP as well as 40 U of RNasin (Promega). The mixtures also contained 2 μl of the *X. laevis* S-100 extract and 8 fmol of a labeled RNA substrate. Following 90 min of incubation at 20°C, the resultant RNA was resolved on a 9 M urea–4% polyacrylamide gel and detected by autoradiography (14). For frog extract competition studies, prior to the 90-min incubation with the RNA substrate, reaction mixtures were preincubated for 60 min with a 40-fold (Fig. 3 and 4) or a 60-fold (Fig. 7) molar excess of competitor RNA. The 25-μl mouse processing reactions were carried out as described previously (14) with 1.5 μl of the mouse S-100 extract, 8 fmol of a labeled RNA substrate, and a 45-min incubation period at 30°C. Competitor RNAs (40-fold excess) were preincubated with the mouse extract for 20 min at 30°C.

For mobility shift analysis of the assembled nucleoprotein, instead of terminating the processing reaction and isolating the RNA, 800 μg of heparin per ml was added to the reaction mixture, which was incubated for an additional 10 min at 20°C. A 10-μl aliquot was then directly analyzed on a native 4% polyacrylamide gel (acrylamide-bisacrylamide [65:1]) as described previously (14). For sucrose gradient analysis of the assembled nucleoprotein, three normal reaction mixtures treated as for mobility shift analysis, except with 400 μg of heparin per ml, were layered onto a 5-ml 5 to 20% sucrose gradient in a reaction buffer lacking glycerol and ATP but containing 0.5 mM $MgCl_2$ and then sedimented at 50,000 rpm at 20°C in an SW55 rotor for 2.5 h. Twenty-three fractions of 225 μl were collected from the top, and 100 μl of each was subjected to mobility shift analysis.

Micrococcal nuclease and RNase H digestion of the extract and UV cross-linking. Digestions were performed as described previously (15), except that the micrococcal nuclease digestion was done for 2.5 min and the RNase H digestion utilized 5 μl of extract, and was done for 30 min at 30°C and was followed by a 10-min 30°C DNase I digestion. The anti-*X. laevis* U3 oligonucleotide was TTTGTGAGT TCAGAC (residues 73 to 61) (26), and the nonspecific oligonucleotide used in Fig. 5B was CTACCAAATACAAT TAAC.

For UV cross-linking, 4-thiouridine triphosphate (4-S-UTP) was prepared and incorporated into RNA along with the ^{32}P label, and the cross-linking was performed as described previously (14). The reactions were carried out as for in vitro processing, except that NaCl was substituted for KCl and a 60-fold molar excess of competitor RNA was used. Following irradiation and RNase digestion, the proteins were resolved on a 10% polyacrylamide (acrylamide-bisacrylamide [75:1])–sodium dodecyl sulfate (SDS) gel.

RESULTS

To examine whether there is processing within the 5' ETS of *Xenopus* pre-rRNA, we analyzed the 5' ETS region of *X. laevis* cellular rRNA by S1 nuclease mapping. In addition to molecules corresponding to the known transcription initiation site (25, 29), shorter RNAs were also observed (arrow in Fig. 2A). The 5' ends of these shorter molecules map to residues +105 to +107 of the *X. laevis* 5' ETS, relative to a sequence analysis of the S1 nuclease probe DNA (lane 1).

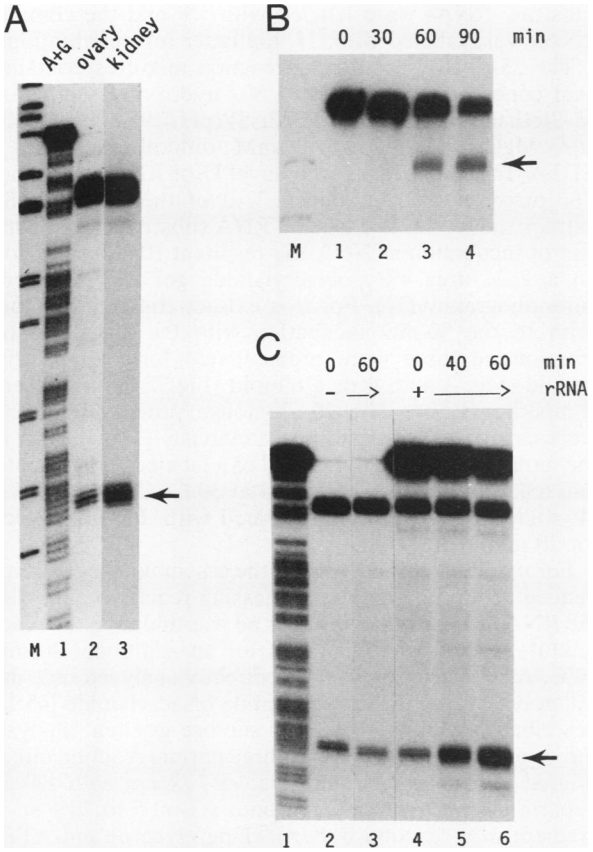

FIG. 2. Processing in the 5′ ETS of *X. laevis* RNA. (A) In vivo RNA. The 5′ ends of cellular RNAs isolated from *X. laevis* ovary cells (lane 2) and cultured kidney cells (lane 3) were mapped by S1 nuclease analysis with a 5′-end-labeled probe. The dark upper band represents RNA that starts at residue +1; the bands indicated by the arrow represent RNAs whose 5′ ends map to residues +105, +106, and +107. Lane 1 is an A+G sequence analysis (17) of the probe DNA (no full-length probe remains in lanes 2 and 3); lane M contains an *Hpa*II-cleaved pBR322 size marker. (B) In vitro processing. ^{32}P-labeled X729 RNA was incubated in a *Xenopus* S-100 processing reaction mixture for the indicated times prior to RNA isolation and electrophoretic analysis. The processed RNA is indicated by the arrow. Lane M shows the 622- and 527-nt fragments from *Hpa*II-cleaved pBR322. (C) In vitro processing. Processing reaction mixtures containing no exogenous RNA (lanes 2 and 3) or containing X293 RNA (lanes 4 to 6; ^{3}H labeled for quantitation) were incubated for the indicated times prior to RNA isolation and S1 nuclease mapping as described for panel A. The probe, prepared from X293 DNA, was completely protected by the input exogenous RNA (the largest band in lanes 4 to 6); the second largest band represents unprocessed cellular RNA that was naturally present in the extract and diverges from the probe upstream of rRNA residue +28; and the shortest bands, indicated by the arrow, represent rRNA processed in vitro and in vivo at residues +105, +106, and +107. Lane 1 is an A+G sequence analysis of the probe DNA.

Since transcription initiation has not been observed in *X. laevis* rDNA at position ~+105 (25, 28), the rRNA beginning at residue +105 may instead be derived from an rRNA processing event.

To assess whether the *X. laevis* 5′ ETS contains an in vitro processing site, T7 RNA polymerase-generated transcripts containing virtually the entire 713-nt 5′ ETS (extending from residue +28 to or beyond residue +729) were incubated in a *Xenopus* kidney cell S-100 extract, and the resultant RNA was electrophoretically analyzed. Over time, one new RNA species arose, and it was ~100 nts shorter than the input molecules, whether they extended to residue +729 (Fig. 2B) or beyond (data not shown), indicative of a processing event at residue ~+105. No other specific cleavage sites were detected in the 5′ ETS. S1 nuclease mapping of unlabeled RNA from such a processing reaction confirmed that the in vitro-generated 5′ ends (Fig. 2C, lanes 5 and 6) precisely coincided with the in vivo ~+105 RNA contributed by the small amount of cellular rRNA present in the S-100 extract (Fig. 2C, lanes 2 to 4). Since this in vitro processing site corresponds to an in vivo-generated rRNA end, it is evidently a true *Xenopus* rRNA processing site.

A similar analysis performed on *X. borealis* cellular rRNA indicated that the primary ribosomal transcript of this species was also processed at an analogous site (residues +118 and +119 within the 5′ ETS; data not shown). Both the *X. laevis* and *X. borealis* 5′ ETS processing sites are 6 to 7 nts upstream of an ~120-nt block whose sequence is 95% conserved between *X. laevis* and *X. borealis* and is also present in *X. clivii* (Fig. 3A, top), while the surrounding ETS segments show much less sequence conservation. This processing is reminiscent of mammalian 5′ ETS processing, which also occurs 6 to 7 nts upstream of an ~200-nt conserved block that contains the processing signal in its proximal 120 nts (Fig. 3A, bottom) (7). Notably, the first 11 nts of the mammalian conserved sequence include those residues most critical for processing (since small mutations of this region but not of other regions abolish processing [7]), and they are identical at 10 or 11 positions to the first 11 nts of the frog consensus sequence (Fig. 3A) (5). These facts imply a commonality between *Xenopus* processing and mammalian processing.

If *Xenopus* 5′ ETS processing is analogous to that of mammals, one would predict that (i) mutation of the conserved 11-nt sequence of *Xenopus* rRNA should also abolish processing and (ii) sequences downstream of the 120-nt *Xenopus* conserved region should also not be required for processing. We thus prepared plasmids X729Δl and X729Δr, whose transcripts are identical to those of the processing-competent X729 RNA used in Fig. 2B, except that they contain either of two overlapping deletions that together remove the entire conserved 11-nt sequence (see Materials and Methods and Fig. 3B). Neither of these mutant transcripts exhibited in vitro processing (Fig. 3C, lanes 4 and 6), demonstrating a requirement for the frog-mouse conserved sequence in directing frog 5′ ETS processing. A parallel set of shorter rRNA templates that extends only to residue +293 but includes the 120-nt frog conserved region was prepared (Fig. 3B). Transcripts of the short wild-type template, X293, directed processing (Fig. 3C, lane 8; see also Fig. 2C), while transcripts of X293Δl and X293Δr, with deletions of the left and right portions of the critical 11 nts, respectively, did not (Fig. 3C, lanes 10 and 12), consistent with the prediction made above.

The experiments shown in Fig. 4 indicate that the processing-competent *X. laevis* substrates sequester an extract component(s) that is essential for the processing reaction. First, the ability or inability of various frog rRNAs to compete in a processing reaction was found to parallel their ability or inability to direct processing (Fig. 4A). Preincubation of the extract with processing-competent X729 or X293 RNA or with an *X. borealis* rRNA transcript abolished the processing of subsequently added radiolabeled X729 RNA (lanes 3 and 7 and data not shown). In contrast, preincubation with processing-incompetent X729Δl, X729Δr, X293Δl,

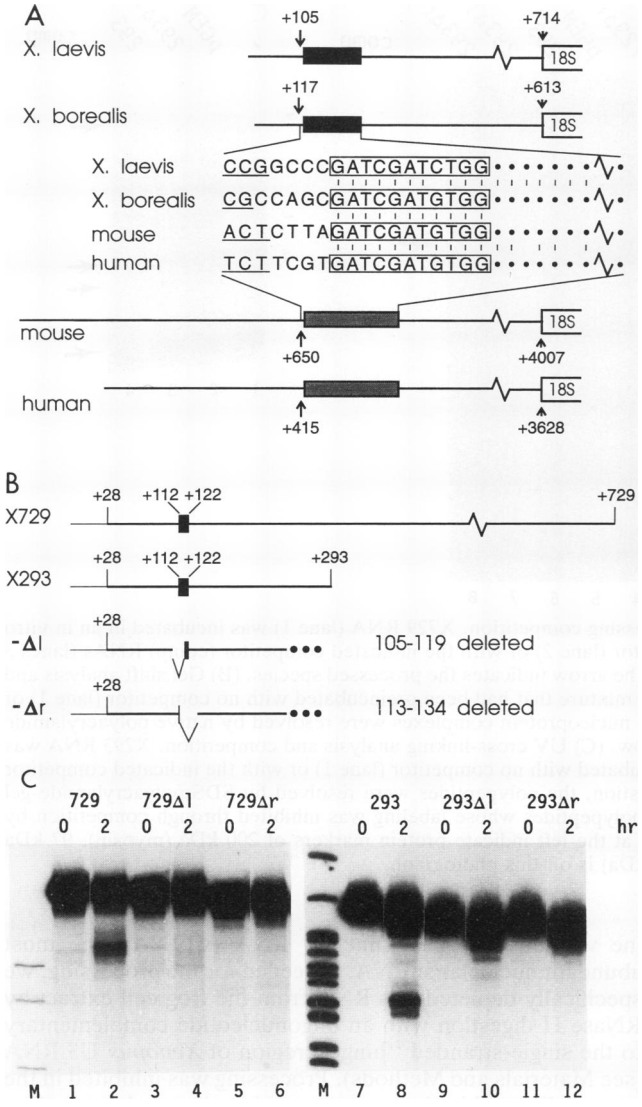

FIG. 3. Conserved sequence domains critical in directing ETS processing. (A) 5' portion of *X. laevis*, *X. borealis*, mouse, and human rRNAs. The solid and stippled boxes denote the 120- and 200-nt segments that are conserved in frog rRNA and in mammalian rRNA, respectively; the first 11 nts of these segments are conserved between frogs and mammals (boxed residues in the middle diagram; see also reference 5). The *X. laevis-X. borealis* conserved sequence was noted in reference 10. The sequenced region of *X. clivii* rRNA (1) also shows this conserved sequence, and *X. clivii* is identical to *X. borealis* in the boxed 11 nts. The conserved sequence block in mouse and human rRNAs was reported in reference 13, while that in rat rRNA was reported in reference 5. The largest major processed fragment starts at the residue indicated by the arrow to the left of the boxed segment. Processed RNAs 1 or 2 nts shorter at the 5' end were also observed (Fig. 2) (13); all the detected major 5' ends of the processed rRNAs are indicated by underlining in the middle diagram. The first residue found in the 18S region is indicated to the left of the 18S segment. Vertical lines indicate sequence identity; dots indicate additional nucleotides. (B) rRNA substrates. The in vitro RNA transcripts of X729 and X293 and their Δl and Δr derivatives are diagrammed. The thin line to the left of rRNA residue +28 represents a short T7 promoter-polylinker sequence at the 5' end of each transcript. (C) In vitro processing. RNAs transcribed from X729 and its Δl and Δr derivatives (lanes 1 to 6) and from X293 and its Δl and Δr derivatives (lanes 7 to 12) were incubated in the in vitro processing reaction mixture for 0 or 2 h as indicated and analyzed as described in the legend to Fig. 2A. Lane M contains an *Hpa*II-cleaved pBR322 marker. The processed products from X729 and X293 RNAs migrated slightly more slowly than the 622- and 160-nt markers, respectively, while the unprocessed X293 RNA migrated slightly faster than the 309-nt marker. The gels of lanes 1 to 6 and 7 to 12 were run to different extents.

or X293Δr RNA or with pGEM RNA did not (lanes 4 to 6 and 8 and 9). Thus, processing-competent RNAs compete for an extract component(s) that is essential for processing, while processing-incompetent RNAs do not compete for such an essential limiting component.

Gel shift analysis then confirmed that components of the processing extract specifically bind to processing-competent substrate RNAs. When incubated with a frog cell extract, X293 RNA directed the formation of a complex that migrated slowly in native polyacrylamide gels (arrow in Fig. 4B, lane 1), while processing-incompetent X293Δl and X293Δr RNAs did not generate such a complex (data not shown). The sequence specificity of the slowly migrating X293 complex was demonstrated by its competition when the extract was preincubated with unlabeled processing-competent X729 and X293 RNAs but not when it was similarly preincubated with processing-incompetent Δl and Δr derivative RNAs or with pGEM RNAs (Fig. 4B).

To identify protein components of the frog cell extract that specifically and directly bound the processing-competent RNA, we used UV cross-linking–label transfer analysis. Radiolabeled and 4-S-U-substituted X293 RNA was incubated in a frog cell extract that had been preincubated with no RNA or with unlabeled processing-competent or processing-incompetent competitor RNAs. Following treatment with UV light to induce cross-linking, the reaction mixtures were treated with RNases to remove all but one or a few nucleotides at the sites of the cross-links, and finally the proteins tagged because of the label transfer were electrophoretically resolved and visualized by autoradiography. X293 RNA selectively bound and transferred label to extract polypeptides (Fig. 4C). Those of about 196, 77, 67, and 51 kDa (arrows in Fig. 4C) were bound in a sequence-specific manner because their labeling was inhibited through competition by preincubation of the extract with processing-competent RNA (lane 4) but not processing-incompetent RNA (lanes 2 and 3 and data not shown). Furthermore, these four polypeptides appear to bind in association with each other, since the relatively small Δ1 and Δr deletions of critical residues abolished interactions with all of them. Similarly, in the mouse 5' ETS processing system, a small deletion of critical residues also abolished UV cross-linking to all six specifically binding polypeptides (14).

We next wanted to examine the size of the multicomponent complex that assembled on the processing-competent RNA. The sedimentation coefficient of this complex on X293 RNA was measured by sucrose gradient velocity centrifugation and found to be ~20S (data not shown). Notably, the mouse ETS processing complex is also ~20S (14).

Because all the features described above for the *Xenopus* 5' ETS processing complex are highly reminiscent of those of mammalian 5' ETS processing, we examined whether the frog processing reaction also shows RNA cofactor dependence. 5' ETS processing activity was abolished by pretreatment of the frog extract with micrococcal nuclease (Fig. 5A, lane 3) but not with control mixtures (lane 2 and data not shown), suggesting that a nucleic acid is required. To exam-

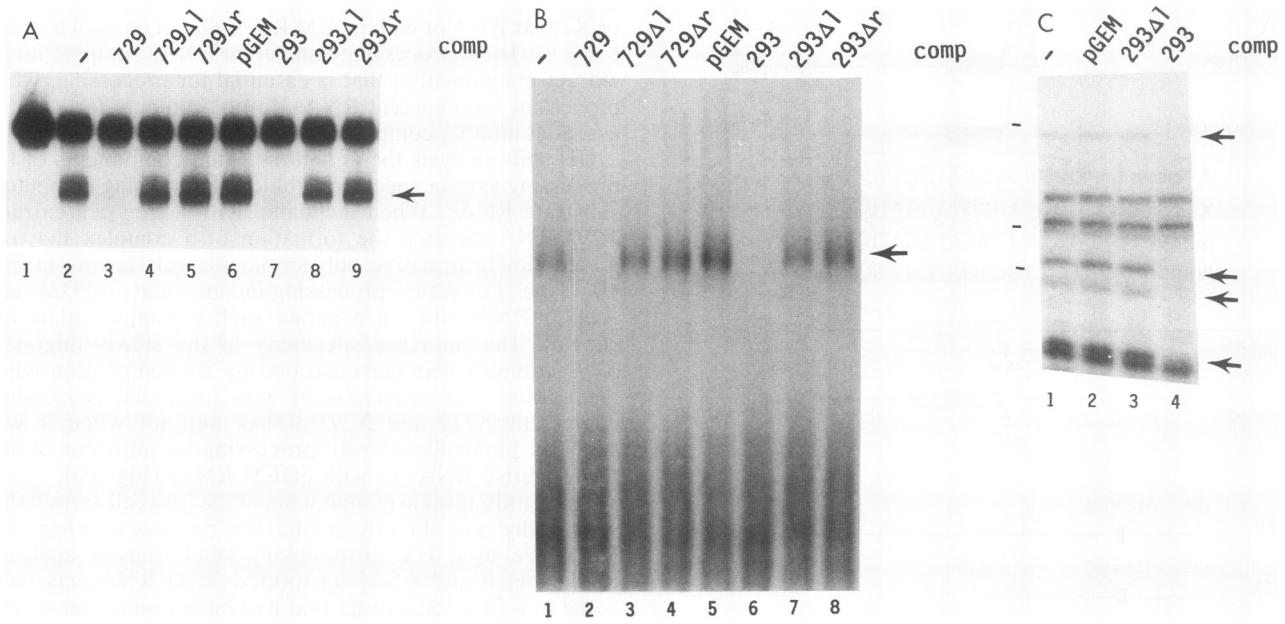

FIG. 4. Complex formation by processing-competent RNA. (A) Processing competition. X729 RNA (lane 1) was incubated in an in vitro processing reaction mixture that had been preincubated with no competitor (lane 2) or with the indicated competitor (comp) RNAs (lanes 3 to 9). The resultant radiolabeled RNA was electrophoretically resolved. The arrow indicates the processed species. (B) Gel shift analysis and competition. X293 RNA was incubated in an in vitro processing reaction mixture that had been preincubated with no competitor (lane 1) or with the indicated competitor (comp) RNAs (lanes 2 to 8). The resultant nucleoprotein complexes were resolved by native polyacrylamide gel electrophoresis. The specific retarded complex is indicated by an arrow. (C) UV cross-linking analysis and competition. X293 RNA was incubated in an in vitro processing reaction mixture that had been preincubated with no competitor (lane 1) or with the indicated competitor (comp) RNAs (lanes 2 to 4). Following UV irradiation and RNase digestion, the polypeptides were resolved by SDS-polyacrylamide gel electrophoresis and detected by autoradiography. The arrows indicate polypeptides whose labeling was inhibited through competition by processing-competent but not processing-incompetent RNAs. The lines at the left indicate protein markers of 200 kDa (myosin), 97 kDa (phosphorylase *b*), and 68 kDa (bovine serum albumin); ovalbumin (43 kDa) is off this photograph.

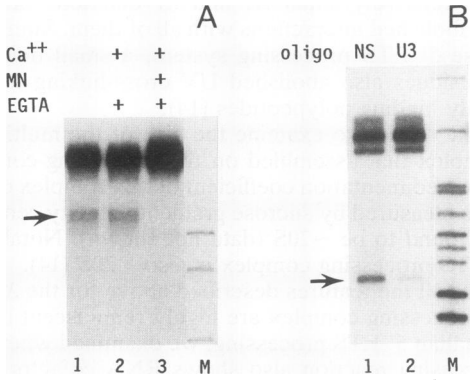

FIG. 5. In vitro processing utilizes U3 snRNA. (A) Micrococcal nuclease digestion. The processing extract was incubated with no additions (lane 1) or with 1 mM $CaCl_2$, micrococcal nuclease (MN) and, 2.5 min later, EGTA as indicated (lanes 2 and 3). These extracts were then used in an in vitro processing reaction with X729 RNA. The processed RNA is indicated by the arrow. Lane M contains an *Hpa*II-cleaved pBR322 marker. (B) RNase H digestion. The processing extract was treated with RNase H in the presence of a nonspecific oligonucleotide (lane 1) or an oligonucleotide complementary to the U3 hinge region (residues 61 to 75; lane 2). (The extract components protected nearly 50% of U3 from the oligonucleotide-RNase H digestion.) These treated extracts were then used to process X293 RNA. The processed RNA is indicated by the arrow. Lane M contains an *Hpa*II-cleaved pBR322 marker.

ine whether U3 small nuclear RNA (snRNA), the most abundant nucleolar snRNA, is needed for the processing, we specifically depleted this RNA from the frog cell extract by RNase H digestion with an oligonucleotide complementary to the single-stranded "hinge" region of *Xenopus* U3 RNA (see Materials and Methods). Processing was inhibited in the extract digested in the presence of this oligonucleotide (Fig. 5B, lane 2) but not in the extracts digested in the presence of nonspecific oligonucleotides (lane 1 and data not shown). Thus, the *Xenopus* 5′ ETS processing reaction appears to be identical to that of mice in its U3 requirement as well.

Since 5′ ETS processing in *X. laevis* appears so similar to that in mice, we examined whether the processing signals in these two species could be functionally exchanged. When the *X. laevis* pre-rRNA substrate was incubated with the kind of mouse cell S-100 extract that we used for the processing of mouse pre-rRNA, the frog rRNA was indeed processed (Fig. 6A, left lane). No processing was detected with the Δl or Δr derivatives of the frog rRNA, reproducing the sequence specificity shown with the homologous frog extract (data not shown). Furthermore, S1 nuclease mapping of the heterologously processed frog rRNA confirmed the use of the same processing site as that used in the homologous frog extract (Fig. 6B; see also Fig. 2C). Thus, the frog 5′ ETS processing signal is faithfully recognized and acted on by mouse cell factors.

The heterologous processing of frog pre-rRNA in the mouse cell extract utilizes factors in common with those utilized in the homologous processing of mouse pre-rRNA in that extract, because the processing of mouse RNA (Fig. 6C,

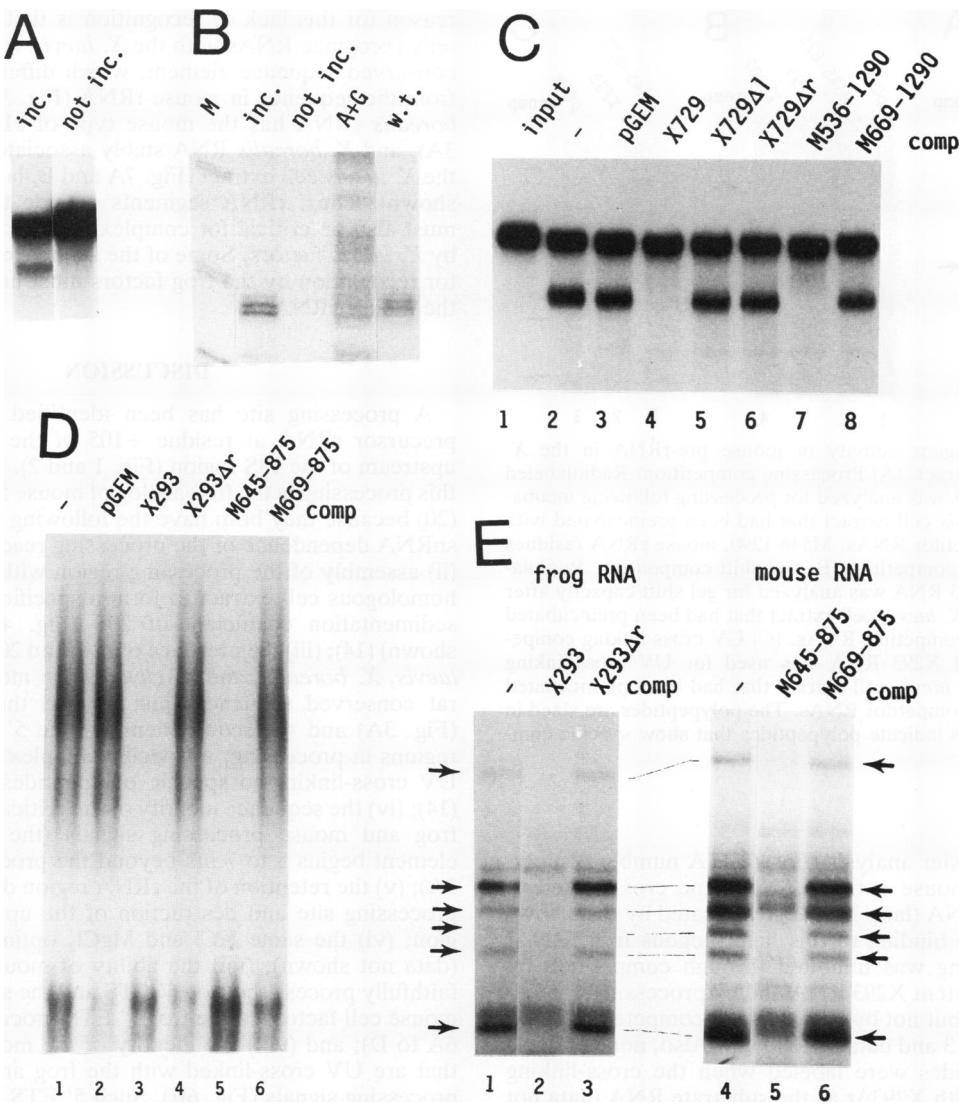

FIG. 6. Heterologous activity of *X. laevis* pre-rRNA in a mouse cell S-100 extract. (A) Processing reaction. X729 RNA was incubated (inc.) or not incubated (not inc.) with the mouse cell S-100 extract, and the products were electrophoretically resolved. X293 RNA was similarly processed. (B) S1 nuclease mapping. The 5' end of X729 RNA that was incubated or not incubated with the mouse S-100 extract was mapped by S1 nuclease analysis as described in the legend to Fig. 2A. Lane w.t. shows a similar S1 nuclease analysis of *X. laevis* ovary RNA. Lane A+G shows an A+G ladder of the probe DNA; the marker bands lane M are the 67-, 76-, and 90-nt fragments of *Hpa*II-cleaved pBR322. (C) Processing competition. Radiolabeled mouse rRNA (residues 546 to 1294) (lane 1) was reacted with a mouse cell extract that had been preincubated without competitor RNA (lane 2) or with the indicated unlabelled *X. laevis* (lanes 4 to 6) or mouse (lanes 7 and 8) competitor RNAs (comp), and the resultant RNA was electrophoretically analyzed. Mouse rRNA starting at or before residue 645 is processing competent; that starting at or beyond residue 669 is processing incompetent. (D) Gel shift competition. Radiolabeled mouse rRNA (residues 645 to 875) was analyzed for gel shift capacity after incubation with a mouse cell extract that had been preincubated without a competitor (lane 1) or with the indicated unlabeled pGEM (lane 2), frog (lanes 3 and 4), and mouse (lanes 5 and 6) competitor RNAs. (E) UV cross-linking analysis and competition. Radiolabeled *X. laevis* RNA X293 (lanes 1 to 3) or mouse rRNA (residues 645 to 875) (lanes 4 to 6) was used for UV cross-linking analysis with a mouse cell extract that had been preincubated without a competitor (lanes 1 and 4) or with the indicated unlabeled competitor RNAs (lanes 2, 3, 5, and 6) as described in the legend to Fig. 4C. The specifically cross-linked polypeptides of about 250, 110, 95, 85, 75, and 52 kDa (14) are indicated by arrows.

lane 2) was inhibited when the mouse cell extract was preincubated with processing-competent frog or mouse RNA (lanes 4 and 7) but not processing-incompetent RNA (lanes 5, 6, and 8). Titration of such processing competition shows the frog RNA to be ~20-fold less effective a competitor than the homologous mouse RNA (data not shown). Nonetheless, it is not only a soluble processing component(s) that is used in common between the two substrate RNAs. Figure 6D shows that mouse cell extract components that bind to the mouse rRNA to form the gel shift complex are specifically removed by competition with processing-competent frog RNA as well as mouse RNA (lanes 3 and 5) but not with processing-incompetent RNA (lanes 4 and 6).

The extent to which mouse cell factors bind to both the homologous mouse substrate RNA and the heterologous frog substrate RNA was directly assessed by UV cross-

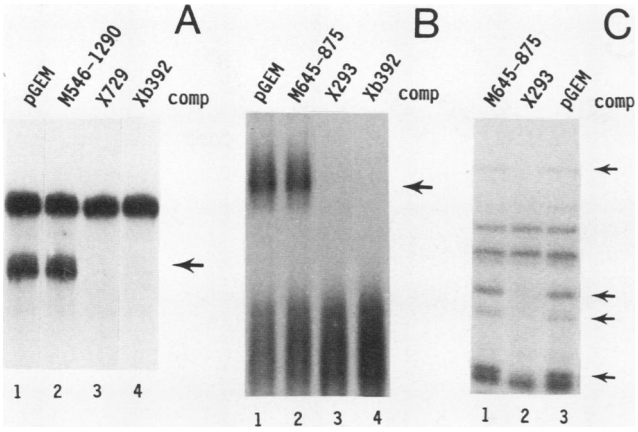

FIG. 7. Heterologous activity of mouse pre-rRNA in the *X. laevis* cell S-100 extract. (A) Processing competition. Radiolabeled *X. laevis* X729 RNA was analyzed for processing following incubation with an *X. laevis* cell extract that had been preincubated with the indicated competitor RNAs. M546-1290, mouse rRNA residues 546 to 1290. comp, competitor. (B) Gel shift competition. Radiolabeled *X. laevis* X293 RNA was analyzed for gel shift capacity after incubation with an *X. laevis* cell extract that had been preincubated with the indicated competitor RNAs. (C) UV cross-linking competition. Radiolabeled X293 RNA was used for UV cross-linking analysis with an *X. laevis* cell extract that had been preincubated with the indicated competitor RNAs. The polypeptides are sized in Fig. 4C. The arrows indicate polypeptides that show specific competition.

linking–label transfer analysis (Fig. 6E). A number of polypeptides of the mouse extract did become cross-linked to X293 substrate RNA (lane 1). Those indicated by the arrows represent specific binding to this heterologous frog rRNA, since their labeling was inhibited through competition by processing-competent X293 RNA and by processing-competent mouse RNA but not by processing-incompetent X293Δr RNA (lanes 2 and 3 and data not shown). Also, none of these specific polypeptides were labeled when the cross-linking was performed with X293Δr as the substrate RNA (data not shown). Notably, these specifically labeled mouse polypeptides coincided with those that were specifically labeled when the homologous mouse rRNA was used as a substrate (lanes 4 to 6 and data not shown). Furthermore, the labeling of the mouse polypeptides with mouse rRNA was inhibited through competition by preincubation with processing-competent frog rRNA (data not shown). The facts (i) that the same-sized mouse polypeptides were labeled with frog rRNA as with mouse rRNA and (ii) that mouse rRNA competed with the labeling of these polypeptides on frog rRNA and vice versa indicate that the 5′ ETS processing complexes formed on the substrates of these two species utilize the same basic polypeptide complex.

Since the frog 5′ ETS processing signal is faithfully recognized by the mouse cell extract, one might anticipate that the converse would also be true. However, the mouse 5′ ETS processing substrate was not processed in the *X. laevis* cell extract, nor did it form a specific complex in the frog cell extract that was detectable by gel shift analysis or by UV cross-linking; this mouse substrate RNA also did not act as a competitor in a frog processing reaction, gel shift analysis, or UV cross-linking reaction (Fig. 7 and data not shown). Thus, *X. laevis* factors do not detectably recognize the mouse 5′ ETS processing signal. One could propose that the reason for this lack of recognition is that *X. laevis* factors only recognize RNAs with the *X. laevis* version of the 11-nt conserved sequence element, which differs at one position from the sequence in mouse rRNA (Fig. 3A). However, *X. borealis* rRNA has the mouse type of 11-nt element (Fig. 3A), and *X. borealis* RNA stably associated with factors in the *X. laevis* cell extract (Fig. 7A and B, lane 4, and data not shown). Thus, rRNA segments outside the 11-nt element must also be critical for complex formation and processing by *X. laevis* factors. Some of the sequence elements needed for recognition by the frog factors must not be provided by the mouse rRNA.

DISCUSSION

A processing site has been identified in the *X. laevis* precursor rRNA at residue +105 of the 5′ ETS, 600 nts upstream of the 18S region (Fig. 1 and 2). We conclude that this processing is the frog analog of mouse 5′ ETS processing (20) because they both have the following properties: (i) U3 snRNA dependence of the processing reaction (Fig. 5) (15); (ii) assembly of the processing region with factors from the homologous cell extract to form a specific complex, with a sedimentation coefficient of 20S (Fig. 4A and data not shown) (14); (iii) the presence of 120- and 200-nt regions in *X. laevis*, *X. borealis*, and *X. clivii* and in mouse, human, and rat conserved sequences just beyond the processing site (Fig. 3A) and the requirement for the 5′ portion of these regions in processing, in specific complex assembly, and in UV cross-linking to specific polypeptides (Fig. 3C and 4) (14); (iv) the sequence identity of the critical 5′ portion of the frog and mouse processing signals (the conserved 11-nt element begins 5 to 7 nts beyond the processing sites; Fig. 3A); (v) the retention of the rRNA region downstream of the processing site and destruction of the upstream rRNA region; (vi) the same KCl and $MgCl_2$ optima for processing (data not shown); (vii) the ability of mouse cell factors to faithfully process the frog 5′ ETS and the specific binding of mouse cell factors to the frog 5′ ETS processing signal (Fig. 6A to D); and (viii) the identity of the mouse polypeptides that are UV cross-linked with the frog and mouse 5′ ETS processing signals (Fig. 6E). Such 5′ ETS processing therefore is not restricted to mammals but instead occurs over a larger range of organisms, extending at least through amphibians.

The ability of the mouse cell processing factors to recognize, stably bind to, and act on the frog rRNA processing signal attests to these processing recognitions being well conserved in vertebrate evolution. It is especially notable that UV cross-linking studies identified the same set of six mouse polypeptides binding specifically to the mouse and frog 5′ ETS processing signals and that even their relative labeling efficiencies were quite similar when rRNAs from the two species were used (Fig. 6E). The one difference in relative UV labeling efficiency (a reduced intensity for the fourth largest polypeptide when frog rRNA was used) could be due to a small structural difference between the two processing complexes or merely could reflect an rRNA sequence difference; i.e., the 4-S-U residue adjacent to a labeled C residue in mouse rRNA whose cross-linking caused most of the labeling of this polypeptide is not present in the frog rRNA sequence.

It is also clear that 5′ ETS processing components are not fully conserved in vertebrate evolution. Notably, the polypeptides identified by UV cross-linking as specifically associated with the processing signals differ between frog and

mouse cell extracts in size and evidently also in number (Fig. 4C and 6E). In addition, the mouse processing signal is not recognized by the *X. laevis* cell factors, either for processing or for complex formation (Fig. 7). It is interesting that the direction in which the heterologous mouse-frog 5' ETS processing functions (frog rRNA with mouse factors, but not mouse rRNA with frog factors) mirrors the situation for heterologous rDNA transcription, in which *X. laevis* rDNA is specifically transcribed by mouse factors, while mouse rDNA is not transcribed by frog factors, both in vitro and in vivo (21; unpublished observations).

It remains to be determined precisely what rRNA segments are required for 5' ETS processing complex formation. It is clear that the 11-nt conserved element (*X. laevis* rRNA residues 112 to 122; mouse rRNA residues 657 to 667) is of paramount importance. Not only did the Δ1 and Δr deletions of *X. laevis* abolish complex formation (Fig. 3), but a sequence replacement of this 11-nt element of mouse rRNA also abolished processing (residues 655 to 669 replaced; 7), as did a 3-nt replacement within this element (15a). In contrast, sequence replacements of regions flanking this element, such as of mouse rRNA residues 645 to 653 or 666 to 674, did not abolish processing (7). Since the secondary structure predicted (37) for the 11-nt critical elements in various processing-competent mouse rRNAs are rather different (7), the 11-nt element discussed here is most likely recognized in a single-stranded configuration. Consistent with this hypothesis, placing the mouse 11-nt element in a stable duplex structure abolished processing and complex formation (7). However, the data in Fig. 7B show that residues outside the 11-nt element are also important for complex formation.

The U3 snRNP has now been found to be important for two different rRNA processing events in *Xenopus* species (Fig. 1), one in the 5' ETS (Fig. 5) and the other at the 5' end of the 5.8S region (26). Its role in 5' ETS processing evidently reflects a direct involvement, since this U3 requirement is seen in vitro with a small substrate RNA (Fig. 5B) and since U3 binds this region of the 5' ETS in vivo in *Xenopus* species (21a, 28), as well as in humans (16) and rats (31). For the 5.8S processing site, the U3 requirement could be either direct or indirect, since the data showed that a reduction in U3 levels in vivo caused an altered abundance of a processing intermediate of the large cellular pre-rRNA (26), but the 5' ETS processing complex normally forms considerably before this processing event occurs (21b, 22). Further studies will be needed to determine whether U3 is required for the actual cleavage at the 5.8S boundary or for an earlier event, such as favoring proper folding or positioning of the rRNA substrate, that may facilitate this cleavage in vivo.

Since 5' ETS processing that forms a large complex and requires U3 is conserved between mammals and amphibians, it seems likely that such processing may occur in other organisms as well. In fact, in a number of more distantly related species, a 5' ETS processing event either has been shown (*Neurospora* species [34] and yeast cells [12]) or has been suggested to occur (*Physarum polycephalum* [4], *Tetrahymena pyriformis* [32], *Bombyx mori* [9], maize [18], wheat [2], and pea [24]). The possible involvement of either the U3 snRNP or a large processing complex has not been examined in any of these cases except yeast cells, in which the U3 snRNA is required for processing (12). Although none of the available rRNA sequences for these species show a close replica of the 11-nt mammalian-amphibian conserved element, these species are all rather distant from vertebrates, so this result may not be surprising. We speculate that the 5' ends of all these rRNAs will be the result of 5' ETS processing events and that these processing events will involve a large complex, will require U3, and will be otherwise analogous to those of mice and frogs.

In studies complementary to the present report, we recently showed that the *Xenopus* 5' ETS processing complex is a sizable structure that is readily observed by electron microscopy and in fact has been known for over two decades (22). When visualized by the Miller spreading technique (21), transcribing ribosomal chromatin is known to form a Christmas tree-like structure, with a DNA "trunk" from which extend closely packed nascent ribonucleoprotein "branches" of increasing length, the 5' ends of which are decorated with "terminal balls" (21, 22). By oocyte microinjection, these *Xenopus* rRNA terminal balls have now been demonstrated to be the 5' ETS processing complex defined in this study (22). Data indicate that analogous terminal balls observed in ribosomal chromatin spreads from mice and hamsters are also the cytological visualization of the 5' ETS processing complexes of those species (22). In fact, such terminal balls have been reported for scores of eukaryotic species (unicellular, multicellular, animal, and plant; reviewed in reference 22), and almost certainly all of these balls represent similar 5' ETS processing complexes that form on the ribosomal transcripts of these various species. This idea in turn indicates that 5' ETS processing complex formation is very highly conserved in eukaryotic evolution. Furthermore, since the terminal balls are ubiquitously observed on nascent ribosomal transcripts (whose total synthesis takes <10 min to complete) and generally are already observed on very short nascent ribosomal transcripts, these 5' ETS processing complexes must assemble rapidly in all these species.

In contrast to the wide evolutionary conservation of rapid 5' ETS processing complex formation, the fraction of steady-state precursor rRNA molecules that are processed at the 5' ETS processing site appears to vary greatly among different species and cell types. The processed rRNA comprises ~90% of steady-state precursor rRNA in mouse tissue culture cells (20), ~50% in human tissue culture cells (13), ~30% in *Xenopus* tissue culture cells (Fig. 2) and in *Xenopus* follicle cells (data not shown), and ~1% in *Xenopus* oocytes (22). It should be noted that there is no evidence that the processing pathways of all *Xenopus* pre-rRNA molecules even involve cleavage at the 5' ETS processing site. However, it is clear that the 5' ETS processing signal of all the pre-rRNA molecules rapidly assembles the observed complex (20). It may well be that what is conserved in evolution is not the act of 5' ETS processing per se but rather the rapid formation of a complex of processing factors at the 5' end of the pre-rRNA.

The facts that (i) the signal for 5' ETS processing complex formation is functionally conserved between mammals and amphibians, while most of the 5' ETS region evolves very rapidly, and that (ii) 5' ETS processing complex formation appears to be conserved across all eukaryotes (22) indicate that this 5' ETS processing complex has been selected for in evolution. Because this processing occurs in a spacer region of the pre-rRNA and the flanking RNA will ultimately be destroyed, its role cannot be to create an end of a mature RNA of the ribosome. One possibility for the advantageous function of the complex formed on the 5' ETS processing site is that it aids in later pre-rRNA maturation steps. Consistent with this proposal, a site needed for U3 binding in the 5' ETS of yeast cells (and presumably also needed for 5'

ETS processing) is required in vivo for the processing of the 18S segment (3). Further study will determine whether the role of the mammalian-amphibian 5′ ETS processing complex is to initially sequester components that will then be used at downstream rRNA processing sites.

ACKNOWLEDGMENTS

We are indebted to Brian McStay and Ron Reeder for *Xenopus* cell S-100 extract and to Don Brown and Eddie Jordan for *Xenopus* cell cultures. We also thank Joan Steitz, Mike Wormington, Louise Pape, Nessly Craig, Cathy Enright, and other members of the Sollner-Webb laboratory for helpful discussions and Ken Piller and Nick Theodorakis for helpful reading of the manuscript. We also acknowledge Mary Bonkowski for help in the preparation of the manuscript.

This work was supported by ACS grant NP731.

REFERENCES

1. **Bach, R., B. Allet, and M. Crippa.** 1981. Sequence organization of the spacer in the ribosomal genes of Xenopus clivii and Xenopus borealis. Nucleic Acids Res. **9**:5311–5330.
2. **Barker, R. F., N. P. Harberd, M. G. Jarvis, and R. B. Flavell.** 1988. Structure and evolution of the intergenic region in a ribosomal DNA repeat unit of wheat. J. Mol. Biol. **210**:1–17.
3. **Beltrame, M., and D. Tollervey.** 1992. Identification and functional analysis of two U3 binding sites on yeast pre-ribosomal RNA. EMBO J. **11**:1531–1542.
4. **Blum, B., G. Pierron, T. Seebeck, and R. Braun.** 1986. Processing in the external transcribed spacer of ribosomal RNA from Physarum polycephalum. Nucleic Acids Res. **14**:3153–3166.
5. **Bourbon, H., B. Michot, N. Hassouna, and J. P. Bachellerie.** 1988. Sequence and secondary structure of the 5′ external transcribed spacer of mouse pre-rRNA. DNA **7**:181–191.
6. **Craig, N., S. Kass, and B. Sollner-Webb.** 1987. Nucleotide sequence determining the first cleavage site in the processing of mouse precursor ribosomal RNA. Proc. Natl. Acad. Sci. USA **84**:629–633.
7. **Craig, N., S. Kass, and B. Sollner-Webb.** 1991. Sequence organization and RNA structural motifs directing the mouse primary rRNA processing event. Mol. Cell. Biol. **11**:458–467.
8. **Forsheit, A. B., N. Davidson, and D. D. Brown.** 1974. An electron microscope heteroduplex study of the ribosomal DNAs of Xenopus laevis and Xenopus mulleri. J. Mol. Biol. **90**:301–314.
9. **Fujiwara, H., and H. Ishikawa.** 1987. Structure of the Bombyx mori rDNA: initiation site for its transcription. Nucleic Acids Res. **15**:1245–1258.
10. **Furlong, J. C., J. Forbes, M. Robertson, and B. E. H. Madden.** 1983. The external transcribed spacer and preceding region of Xenopus borealis rDNA: comparison with the corresponding region of Xenopus laevis rDNA. Nucleic Acids Res. **11**:8183–8196.
11. **Gurney, T.** 1985. Characterization of mouse 45S ribosomal RNA subspecies suggests that the first processing cleavage occurs 600 ± 100 nucleotides from the 5′ end and the second 500 ± 100 nucleotides from the 3′ end of a 13.9 kb precursor. Nucleic Acids Res. **13**:4905–4919.
12. **Hughes, J. M. X., and M. Ares, Jr.** 1991. Depletion of U3 small nucleolar RNA inhibits cleavage in the 5′ external transcribed spacer of yeast pre-ribosomal RNA and impairs formation of 18S ribosomal RNA. EMBO J. **10**:4231–4239.
13. **Kass, S., N. Craig, and B. Sollner-Webb.** 1987. The primary processing of mammalian rRNA involves two adjacent cleavages and is not species specific. Mol. Cell. Biol. **7**:2891–2898.
14. **Kass, S., and B. Sollner-Webb.** 1990. The first pre-rRNA processing event occurs in a large complex: analysis by gel retardation, sedimentation, and UV cross-linking. Mol. Cell. Biol. **10**:4920–4931.
15. **Kass, S., K. Tyc, J. Steitz, and B. Sollner-Webb.** 1990. The U3 small nucleolar ribonucleoprotein functions in the first step of pre-ribosomal RNA processing. Cell **60**:897–908.

15a. **Kuehl, P., and B. Sollner-Webb.** Unpublished observations.

16. **Maser, R. L., and J. P. Calvet.** 1989. U3 small nuclear RNA can be psoralen crosslinked in vivo to the 5′ external transcribed spacer of pre-ribosomal RNA. Proc. Natl. Acad. Sci. USA **86**:6523–6527.
17. **Maxam, A., and W. Gilbert.** 1977. A new method for sequencing DNA. Proc. Natl. Acad. Sci. USA **74**:560–564.
18. **McMullen, M. D., B. Hunter, R. L. Phillips, and I. Rubenstein.** 1986. The structure of the maize ribosomal DNA spacer region. Nucleic Acids Res. **14**:4953–4968.
19. **McStay, B., and R. H. Reeder.** 1990. An RNA polymerase I termination site can stimulate the adjacent ribosomal gene promoter by two distinct mechanisms in Xenopus laevis. Genes Dev. **4**:1240–1252.
20. **Miller, K., and B. Sollner-Webb.** 1981. Transcription of mouse rRNA genes by RNA polymerase I: in vitro and in vivo initiation and processing sites. Cell **27**:165–174.
21. **Miller, O. L., Jr., and B. Beatty.** 1969. Visualization of nucleolar genes. Science **164**:955–957.

21a. **Mougey, E.** Unpublished observations.

21b. **Mougey, E., and M. O'Reilly.** Unpublished observations.

22. **Mougey, E., M. O'Reilly, Y. Osheim, O. L. Miller, Jr., A. Beyer, and B. Sollner-Webb.** 1993. The terminal balls characteristic of eukaryotic rRNA transcription units in chromatin spreads are rRNA processing complexes. Genes Dev. **7**:1609–1620.
23. **Pape, L., J. Windle, E. B. Mougey, and B. Sollner-Webb.** 1989. The *Xenopus* ribosomal DNA 60- and 81-base-pair repeats are position-dependent enhancers that function at the establishment of the preinitiation complex: analysis in vivo and in an enhancer-responsive system. Mol. Cell. Biol. **9**:5093–5104.
24. **Piller, K. J., S. R. Baerson, N. O. Polans, and L. S. Kaufman.** 1990. Structural analysis of the short length ribosomal DNA variant from Pisum sativum L. cv. Alaska. Nucleic Acids Res. **18**:3135–3145.
25. **Reeder, R. H., B. Sollner-Webb, and H. Wahn.** 1977. Sites of transcription initiation *in vivo* on Xenopus laevis ribosomal DNA. Proc. Natl. Acad. Sci. USA **74**:5402–5406.
26. **Savino, R., and S. Gerbi.** 1990. In vivo disruption of Xenopus U3 snRNA affects ribosomal RNA processing. EMBO J. **9**:2299–2308.
27. **Savino, R., and S. Gerbi.** 1991. Preribosomal RNA processing in Xenopus oocytes does not include cleavage within the external transcribed spacer as an early step. Biochimie **73**:805–812.
28. **Sollner-Webb, B., and S. McKnight.** 1982. Accurate transcription of cloned Xenopus ribosomal RNA genes. Nucleic Acids Res. **10**:3391–3405.
29. **Sollner-Webb, B., and R. H. Reeder.** 1979. The nucleotide sequence of the initiation and termination sites for rRNA transcription in Xenopus laevis. Cell **18**:485–499.
30. **Sollner-Webb, B., K. Tyc, and J. Steitz.** 1993. Ribosomal RNA processing in eukaryotes. *In* R. Zimmerman and A. Dahlberg (ed.), Ribosomal RNA: structure, evolution, processing and function in protein synthesis, in press. CRC Press, New York.
31. **Stroke, I. L., and A. M. Weiner.** 1989. The 5′ end of U3 snRNA can be crosslinked in vivo to the external transcribed spacer of rat ribosomal RNA precursors. J. Mol. Biol. **210**:497–512.
32. **Sutiphong, J., C. Matzura, and E. G. Niles.** 1984. Characterization of a crude selective Pol I transcription system from Tetrahymena pyriformis. Biochemistry **23**:6319–6327.
33. **Tower, J., S. Henderson, K. Dougherty, P. Weijksnora, and B. Sollner-Webb.** 1989. An RNA polymerase I promoter located in the CHO and mouse ribosomal DNA spacers: functional analysis and factor and sequence requirements. Mol. Cell. Biol. **9**:1513–1525.
34. **Tyler, B. M., and N. H. Giles.** 1985. Structure of a Neurospora RNA polymerase I promoter defined by transcription in vitro with homologous extracts. Nucleic Acids Res. **13**:4311–4331.
35. **Wellauer, P. K., and I. B. Dawid.** 1974. Processing of Xenopus laevis ribosomal RNA and structure of single-stranded ribosomal DNA. J. Mol. Biol. **89**:379–395.
36. **Wellauer, P. K., and I. B. Dawid.** 1974. Processing of mouse L-cell ribosomal RNA and variations in the processing pathway. J. Mol. Biol. **89**:397–407.
37. **Zucker, M.** 1989. On finding all suboptimal foldings of an RNA molecule. Science **244**:48–52.